Inhibition of miR-103a-3p suppresses the proliferation in oral squamous cell carcinoma cells via targeting RCAN1

G. ZHANG, Z. CHEN, Y. ZHANG, T. LI, Y. BAO, S. ZHANG*

Department of Stomatology, The Fourth Hospital of Hebei Medical University, Shijiazhuang, Hebei 050011, China

*Correspondence: zhangsx012@163.com

Oral cancer is one of the common cancers worldwide, among which over 90% are oral squamous cell carcinomas (OSCC). MicroRNAs act as critical regulators of cancer development and progression. MiR-103a-3p has been reported to be upregulated in OSCC patients and closely correlated to poor prognosis, yet its roles in the progression of OSCC remain undisclosed. In this study, we knocked down the expression of miR-103a-3p in two OSCC cell lines in vitro, and significantly repressed cell proliferation and cell cycle arrest at the G1 phase were observed, accompanied by decreased proliferating cell nuclear antigen, cyclin D1, cyclin B1 and increased PTEN levels. MiR-103a-3p inhibition also induced apoptosis as evidenced by increased apoptotic cells and upregulated cleaved caspase-9/casapase-3 expression. We established a xenograft model in nude mice and found that miR-103a-3p knockdown also suppressed tumor growth in vivo. Besides, the expression of regulator of calcineurin1 (RCAN1), known as its anti-tumor effect, was negatively correlated with the miR-103a-3p level in OSCC cells. We validated that RCAN1 was a downstream target of miR-103a-3p using the dual-luciferase assay. RCAN1 silencing reversed the cell proliferative inhibition, cell cycle arrest and cell apoptosis induced by miR-103a-3p knockdown. In addition, we found that long non-coding RNA LINC00675 acted as a sponge of miR-103a-3p and promoted the expression of miR-103a-3p targets RCAN1 and PTEN. In summary, miR-103a-3p inhibition represses proliferation and induces apoptosis of OSCC cells through regulating RCAN1, and miR-103a-3p may act as a novel diagnostic marker and therapeutic target for OSCC.

Key words: oral squamous cell carcinoma, miR-103a-3, RCAN1, proliferation, apoptosis

Oral cancer, also called mouth cancer, belongs to the head and neck cancers. Oral cancer remains one of the common cancers around the world and accounts for approximately 4% of all cancer cases [1]. Oral cancer usually occurs in a tongue, mouth floor, lips, gingiva, and salivary glands. It leads to a series of adverse impacts on patients including speech, swallowing function, appearance changes as well as the major symptom: chronic pain [2]. Oral squamous cell carcinoma (OSCC), originate in the squamous cells, is the most common oral cancers and represents more than 90% of all oral cancers [3]. The major risk factors of oral cancer include smoking, alcohol use, human papillomavirus infection, chronic irritation, and chemical agents, which make oral cancer a preventable disease [4]. Owing to the ignorance of patients and misdiagnosis at an early stage, most oral cancer patients are diagnosed at advanced stages, accompanied with distant metastasis to neck, lung, bone, skin, and liver [5]. To date, surgery, radiation therapy and chemotherapy are major treatments for oral cancer, yet the five-year survival

rate of patients with metastasis is only 39% [6]. Thus seeking specific diagnostic biomarkers and a better understanding of underlying mechanisms of oral cancer progression are of utmost significance for oral cancer treatments.

MicroRNAs are an abundant group of small non-coding RNAs that function as post-transcriptional regulators of target genes via base pairing [7]. MicroRNA miR-103a-3p is involved in the development and progression of several cancers including breast cancer, bladder cancer, lung cancer, colorectal cancer, pancreatic cancer, gastric cancer, and mesothelioma [8–14]. MiR-103a-3p has a higher expression in OSCC patients, which is closely correlated to poor prognosis. MiR-103a-3p, miR-18a, miR-92a, and miR-203 are co-expressed in OSCC and may act as prognostic markers for OSCC [15]. However, the exact roles that miR-103a-3p plays in the development and progression of OSCC remains unclear.

Regulator of calcineurin1 (RCAN1), also called Down syndrome critical region 1 (DSCR1) or modulatory calci-

neurin-interacting protein 1 (MCIP1), is an endogenous protein located on chromosome 21 [16]. RCAN1 is involved in a variety of diseases including Down syndrome, Alzheimer's disease, and cardiovascular disease, and it also acts as a critical regulator of cancers [17, 18]. Remarkably, RCAN1 is frequently downregulated in numerous human cancers and the decreased RCAN1 expression is closely correlated to the poor overall survival of cancer patients [17]. Interestingly, patients with Down's syndrome, in which the RCAN1 expression is elevated, showed notably lower cancer incidence [19]. In addition, *RCAN1* is a putative target gene of miR-103a-3p predicted by Targetscan database. Nevertheless, how they interact with each other to affect the malignancies of OSCC has not been elaborated.

In this study, we investigated the effects of miR-103a-3p and RCAN1 on proliferation and apoptosis in OSCC cell lines *in vitro*. *RCAN1* was validated to be a downstream target gene of miR-103a-3p. We also found a novel up-stream long non-coding RNA of miR-103a-3p.

Materials and methods

Cell culture and transfection. Oral cancer cell lines TSCCA, TCA8113, and CAL-27 were purchased from Procell (China). TSCCA and TCA8113 cells were maintained in Roswell Park Memorial Institute (RPMI)-1640 culture medium containing 20% fetal bovine serum (FBS). CAL-27 cells were cultured in Dulbecco's modified eagle medium (DMEM) with 10% FBS. All cell lines were incubated in a humidified incubator with 5% CO_2 at 37°C [20]. Long non-coding RNA LINC00675 sequence was cloned into the pcDNA3.1 vector to obtain the overexpression plasmid. Cells were transfected with NC/miR-103a-3p inhibitor, NC/miR-103a-3p mimics or RCAN1 siRNAs using Lipofectamine 2000 (Invitrogen, USA) according to the manufacturer's instruction [21]. The sequences of RCAN1 siRNAs were as follows: siRCAN1-1: 5'-ATCACTCTCACATACAT-GGAC-3'; siRCAN1-2: 5'-AGTGATATCTTCAGCGAAA-3'; siRCAN1-3: 5'-GTCCATGTATGTGAGAGTGAT-3'.

Quantitative real-time PCR. Total RNAs of cells and tumor tissues were extracted using a commercial RNA extraction kit (TianGen, China). One microgram of total RNA was used for reverse-transcription [22]. RNA levels of miR-103a-3p and LINC00675 were examined by quantitative real-time PCR using SYBR Green (Solarbio, China) and data were analyzed using the $2^{-\Delta\Delta CT}$ method. Human small nuclear RNA U6 and GAPDH were used as internal controls, respectively. Stem-loop RT primers and real-time PCR primers used were as follows: Hsa-miR-103a-3p specific stem-loop primer: 5'-GTTGGCTCT-GGTGCAGGGTCCGAGGTATTCGCACCAGAGC-CAACTCATAG-3'; Hsa-U6 specific stem-loop primer: 5'-GTTGGCTCTGGTGCAGGGTCCGAGGTATTCG-CACCAGAGCCAACAAAATATGG-3'; Hsa-miR-103a-3p-F: 5'-GCGAGCAGCATTGTACAGG-3'; Hsa-miR-103a-

3p-R: 5'-GTGCAGGGTCCGAGGTATTC-3'; Hsa-U6-F: 5'-GCTTCGGCAGCACATATACT-3'; Hsa-U6-R: 5'-GTGC-AGGGTCCGAGGTATTC-3'; Hsa-LINC00675-F: 5'-CACA-AGCACCAAAGTCCTAA-3'; Hsa-LINC00675-R: 5'-CTG-GTCAGTGTCAAAGGGTA-3'; Hsa-GAPDH-F: 5'-GACCT-GACCTGCCGTCTAG-3'; Hsa-GAPDH-R: 5'-AGGAGT-GGGTGTCGCTGT-3'.

Western blot. Cells and tumor tissues were lysed with RIPA buffer (Solarbio, China) containing 1 mM phenyl-methanesulfonyl fluoride. The protein in the supernatant was quantified with a BCA kit (Solarbio, China), fractionated by sodium dodecyl sulfate polyacrylamide gel electrophoresis (SDS-PAGE) and transferred to PVDF membranes (Millipore, USA). After blocking with 5% skim milk, the membranes were incubated with primary antibodies overnight at 4°C. Then membranes were washed with PBS three times and incubated with secondary antibodies for 60 minutes. Afterward, proteins were visualized using ECL reagent (Solarbio, China) and the optical density values were analyzed with Gel-Pro-Analyzer [12]. Primary antibodies used in this study were as follows: RCAN1 antibody (1:1000, D261343, Sangon biotech, China), caspase-9/cleaved caspase-9 antibodies (1:1000, #9508, CST, USA), caspase-3/cleaved caspase-3 antibodies (1:1000, #9668, CST, USA), cyclin D1 antibody (1:500, A0310, Abclonal, China), cyclin B1 antibody (1:500, A2056, Abclonal, China), phosphatase and tensin homolog (PTEN) antibody (1:500, A2056, Abclonal, China), proliferating cell nuclear antigen (PCNA) antibody (1:1000, 10205-2-AP, Proteintech, China) and GAPDH antibody (1:10000, 60004-1-Ig, Proteintech, China). HRP-conjugated goat anti-rabbit IgG (1:3000, SE134, Solarbio, China) and HRP-conjugated goat anti-mouse IgG (1:3000, SE131, Solarbio, China) were used as secondary antibodies.

Cell counting kit-8. TSCCA and TCA8113 cells were seeded in 6-well plates and transfected with miRNA inhibitors or siRNAs. Then cells were collected and seeded in 96-well plates (5×10^3 cells/well) 24 hours after transfection and incubated with 10 μl CCK-8 (Keygen, China) for 2 h [23]. The optical density value at 450 nm was detected at 0 h, 24 h, 48 h, and 72 h after transfection.

Flow cytometry. Cell cycle and apoptosis of TSCCA and TCA8113 cells were detected using flow cytometry. For cell cycle detection, cells were collected and fixed with 70% ethanol at 4°C for 12 hours. Cells were then washed with PBS twice and stained with 25 μl propidium iodide (Beyotime, China) at 37°C for 30 min, followed by flow cytometry detection [24]. For cell apoptosis detection, cells were collected and re-suspended with 195 μl binding buffer. Then cells were stained with 5 μl Annexin V-FITC (Beyotime, China) and 10 μl propidium iodide (Beyotime, China) for 20 min at room temperature, followed by flow cytometry detection [22].

Dual-luciferase assay. The wildtype and mutant type sequences of RCAN1 3'-UTR or LINC00675 fragments containing the miR-130a-3p binding sites were cloned into

plasmid pmirGLO (Promega, USA). Then the pmirGLO plasmids were co-transfected with NC/miR-103a-3p mimics into 293T cells using Lipofectamine 2000 (Invitrogen, USA). Afterward, cells were lysed with 250 μl lysis buffer, incubated with firefly luciferase substrate and renilla luciferase substrate [25]. The binding activity of miR-103a-3p to RCAN1 3'-UTR or LINC00675 was evaluated by measuring the ratio of firefly luciferase to renilla luciferase activities.

Xenograft model. Healthy 5-week-old male BALB/c nude mice were adaptively fed for one week. TCA8113 cells were inoculated in the right flank of nude mice (5×10^6 cells/ mouse) [26]. Mice were randomly divided into two groups a week after inoculation: miR-103a-3p antagomir and NC antagomir groups (n=6). The mice in these two groups were injected with 25 μl 10 nM miR-103a-3p antagomir or equivalent NC antagomir once every three days for six times around the tumor site. Tumor size was measured every three days. Mice were sacrificed 28 days after inoculation and tumor tissues were isolated for subsequent detections. Animal experiments were performed according to the guideline for the care and use of laboratory animals and approved by the Ethics Committee of the Fourth Hospital of Hebei Medical University.

Hematoxylin-eosin staining. Tumor tissues were embedded into paraffin and sliced into 5 μm sections. Then the embedded sections were deparaffinized using gradient ethanol. After staining with hematoxylin for 5 min and eosin for 3 min, the sections were dehydrated in gradient ethanol and sealed with neutral balsam. Typical pictures were captured under a microscope (×200 magnification).

Statistical analysis. All results were presented as mean ± SD. All data were analyzed using GraphPad Prism 7. Statistical significance between mean values was analyzed with Student's t-test (two groups) or one-way ANOVA (three or more groups). The p-value <0.05 was regarded as statistically significant.

Results

Expression levels of miR-103a-3p and RCAN1 in OSCC cell lines. We first measured the level of miR-103a-3p in three OSCC cell lines, and an obviously higher expression of miR-103a-3p was observed in TSCCA and TCA8113 cells compared with CAL-27 cells (Figure 1A). On the contrary, the protein level of RCAN1 was significantly higher in CAL-27 cells than that in TSCCA and TCA8113 cells (Figure 1B). Then we knocked down the expression of miR-103a-3p using the specific miR-103a-3p inhibitor, and a notably decrease of the miR-103a-3p level was detected in both TSCCA and TCA8113 cells (Figure 1C).
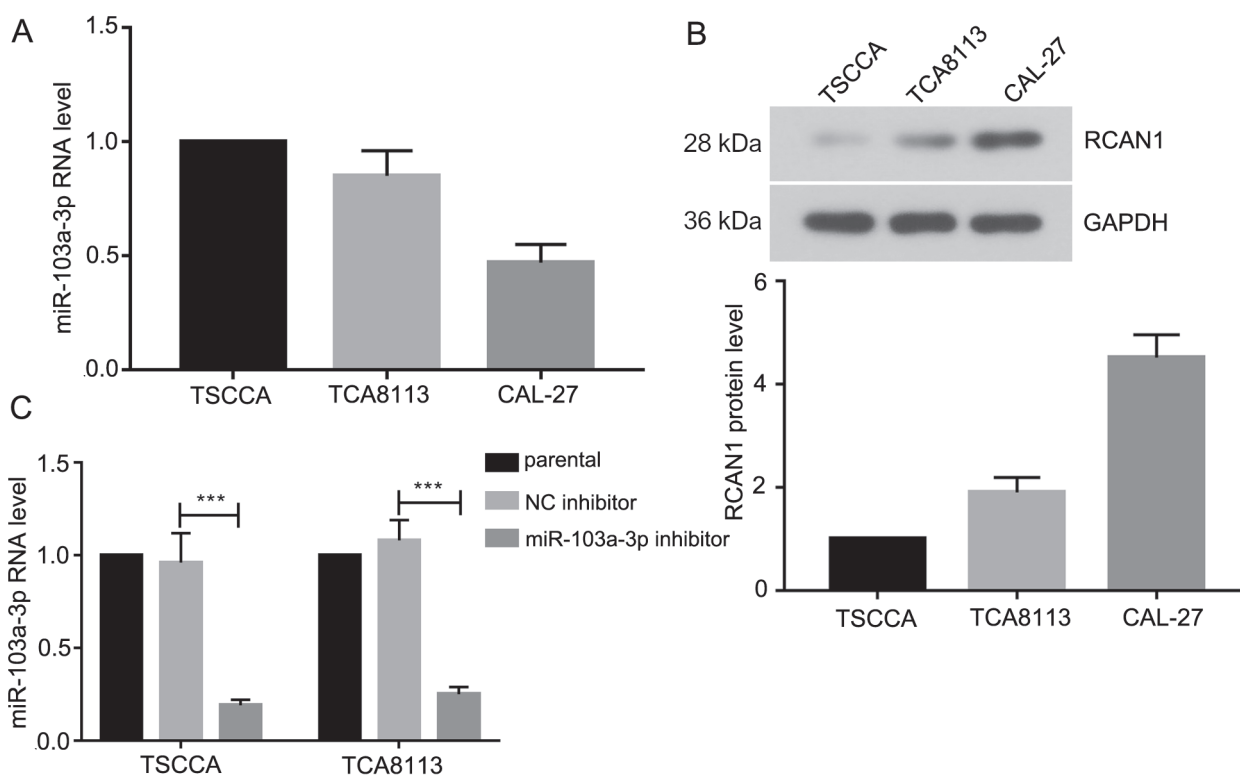

Figure 1. Expression levels of miR-103a-3p and RCAN1 in OSCC cell lines. A) RNA levels of miR-103a-3p in TSCCA, TCA8113, and CAL-27 cells were measured by quantitative real-time PCR. B) Protein levels of RCAN1 in TSCCA, TCA8113, and CAL-27 cells were determined by the western blot assay. C) The efficiency of miR-103a-3p inhibition in TSCCA and TCA8113 cells was evaluated by quantitative real-time PCR. RCAN1: regulator of calcineurin1. OSCC: oral squamous cell carcinoma (OSCC). All data were presented as mean ± SD. ***p<0.001
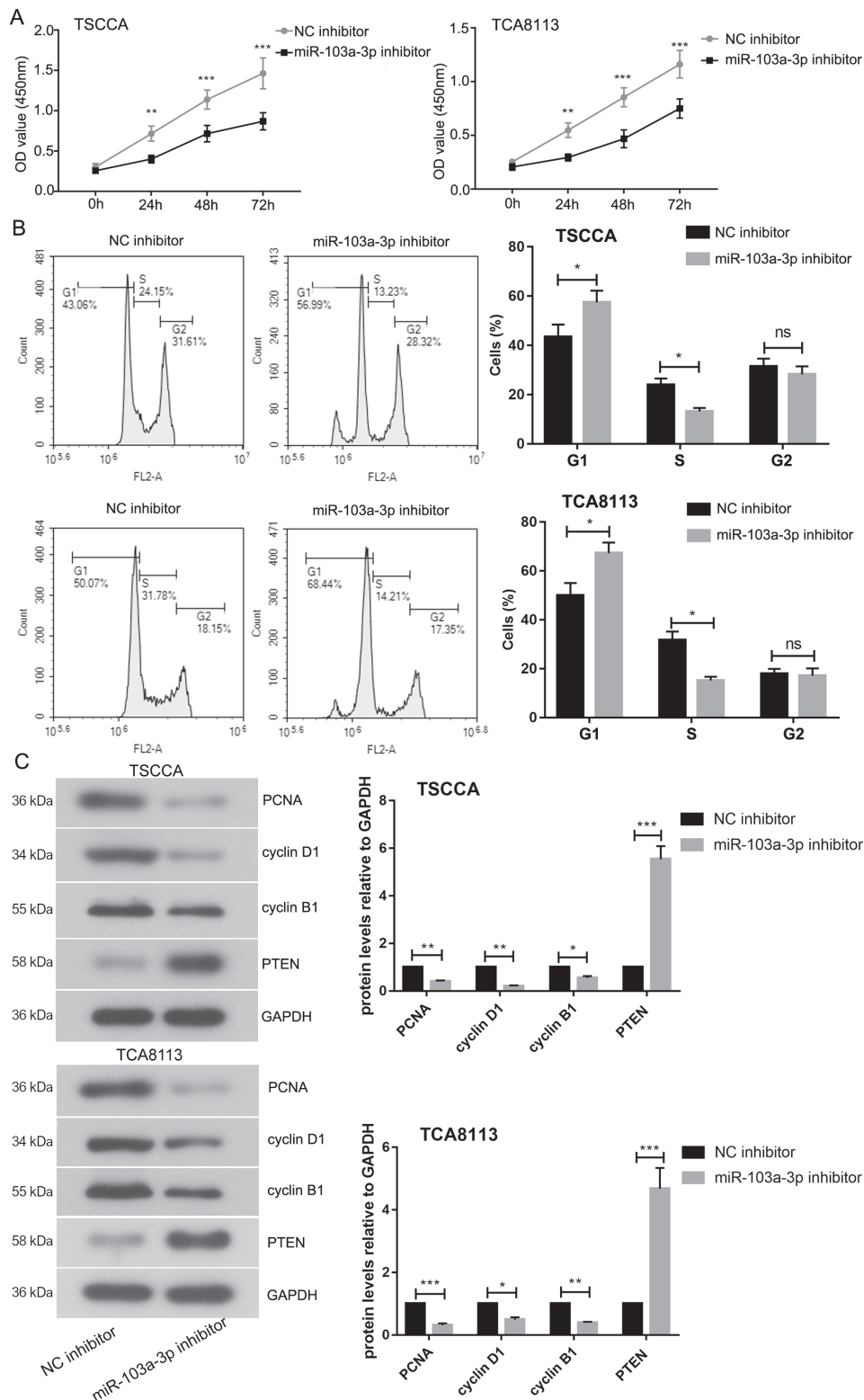
Figure 2. MiR-103a-3p inhibition suppressed the proliferation of OSCC cell lines. A) Proliferation of TSCCA and TCA8113 cells after miR-103a-3p inhibition was assessed by cell counting kit-8 assay. B) TSCCA and TCA8113 cells were stained with propidium iodide, and the cell cycle was detected by flow cytometry assay. C) Protein levels of PCNA, cyclin D1, cyclin B1, and PTEN in TSCCA and TCA8113 cells after miR-103a-3p inhibition were evaluated by western blot assay. PCNA: proliferating cell nuclear antigen. All data were presented as mean ± SD. ns: no significance; *p<0.05; **p<0.01; ***p<0.001

MiR-103a-3p inhibition suppressed proliferation in OSCC cell lines. The cell proliferation of TSCCA and TCA8113 cells was remarkably suppressed 24 hours after miR-103a-3p inhibition (Figure 2A). The cells at the G1 phase were significantly increased while cells at the S phase were remarkably reduced in both TSCCA and TCA8113 cells after miR-103a-3p inhibition (Figure 2B). Further western blot assay showed that miR-103a-3p inhibition reduced PCNA, cyclin D1, and cyclin B1 protein levels, whereas it elevated PTEN protein level in both TSCCA and TCA8113 cells (Figure 2C).

MiR-103a-3p inhibition promoted apoptosis of OSCC cell lines. Next, we investigated the effect of miR-103a-3p inhibition on cell apoptosis in OSCC cell lines. Flow cytometry detection revealed that miR-103a-3p inhibition enhanced cell apoptosis in both TSCCA and TCA8113 cells (Figure 3A). In addition, miR-103a-3p inhibition also upregulated the expression of apoptotic proteins including cleaved caspase-9 and cleaved caspase-3 in both TSCCA and TCA8113 cells (Figure 3B).

RCAN1 was a downstream target of miR-103a-3p. The interaction between miR-103a-3p and RCAN1 was validated using dual-luciferase assay. The results showed that miR-103a-3p mimics significantly inhibited the luciferase activity of the RCAN1-WT but not RCAN1-MUT (Figure 4A). MiR-103a-3p inhibition elevated the RCAN1 protein level in both TSCCA and TCA8113 cells, whereas miR-103a-3p mimics led to a decrease of the RCAN1 protein level in CAL-27 cells (Figure 4B).

MiR-103a-3p regulated proliferation and apoptosis of the OSCC cell line by targeting RCAN1. Next, we knocked down RCAN1 in both TSCCA and TCA8113 cells using specific siRNAs. Western blot assay showed that siRCAN1-2 transfected OSCC cells showed the lowest RCAN1 protein level, thus siRCAN1-2 was used in subsequent experiments (Figure 5A). RCAN1 silencing reversed the proliferative suppression induced by miR-103a-3p inhibition in TSCCA and TCA8113 cells (Figure 5B). MiR-103a-3p inhibition-induced cell cycle arrest was also abolished by RCAN1 silencing (Figure 5C). Further cell apoptosis detection revealed that miR-103a-3p inhibition promoted cell apoptosis, whereas further RCAN1 silencing abrogated the pro-apoptotic effect of miR-103a-3p inhibition in both TSCCA and TCA8113 cells (Figure 5D).

MiR-103a-3p inhibition suppressed tumor growth *in vivo*. Mice were implanted with TCA8113 cells and tumors were injected with NC/miR-103a-3p antagomir to explore the role that miR-103a-3p played in tumor growth. We found that miR-103a-3p antagomir injection significantly suppressed tumor growth compared with control (Figure 6A). Hematoxylin-eosin staining assay demonstrated that miR-103a-3p antagomir promoted cell apoptosis and necrosis in xenograft tumors (Figure 6B). The miR-103a-3p level was significantly decreased in tumor tissues injected with miR-103a-3p antagomir (Figure 6C), whereas the protein level of RCAN1 was elevated (Figure 6D).

LINC00675 acted as a sponge of miR-103a-3p. Further bioinformatic analysis implied that LINC00675 may act as a sponge of miR-103a-3p. Dual-luciferase assay suggested that miR-103a-3p mimics remarkably decreased the luciferase activity of LINC00675-WT, but had no effect on LINC00675-MUT (Figure 7A). Quantitative real-time PCR showed that the RNA level of LINC00675 was significantly lower in both TSCCA and TCA8113 cells than that in CAL-27 cells (Figure 7B). The LINC00675 level was significantly elevated in both TSCCA and TCA8113 cells after pcDNA3.1-LINC00675 transfection (Figure 7C). In addition, the expression levels of two targets of miR-103a-3p, RCAN1 and PTEN, were increased in LINC00675 overexpressed TSCCA and TCA8113 cells, and further miR-103a-3p overexpression decreased the RCAN1 and PTEN levels (Figure 7D).

Discussion

Although oral cancer is a preventable disease, the overall survival of patients is still unsatisfactory as they are diagnosed in advanced stages [6]. Lack of specific biomarkers at an early stage is the major reason for the delayed diagnosis. Expression of microRNAs is tissue/tumor specific, and increasing evidence reveals that aberrant expression of microRNAs is likely to be implicated in the pathogenesis, metastasis, and chemoresistance of oral cancer [27, 28]. In addition, microRNAs are closely correlated to the clinical outcome of oral cancer patients and may serve as biomarkers for oral cancer [29]. For instance, miR-let-7a and miR-181a are downregulated in OSCC and their overexpression inhibits the proliferation of OSCC cells [30, 31]. The upregulation of miR-21, miR-181b, and miR-345 is the feature of oral precancerous lesion cancerization [27]. Furthermore, the aberrantly expressed miR-9, miR-191, and miR-134 can serve as efficient biomarkers for non-invasive oral cancer [32]. In this study, we first investigated the effect of miR-103a-3p, which was upregulated in oral cancer, on the proliferation and apoptosis in OSCC cells.

Cancer cells are characterized by abnormal proliferation beyond its normal life span, which is regulated by a series of cell cycle related proteins including cyclins and cyclin dependent kinases (CDKs) [33]. Cyclin D1 and cyclin B1 are critical regulators of cell cycle progression, and they are aberrantly overexpressed in OSCC and may serve as specific markers of OSCC oncogenesis [34, 35]. PTEN is downregulated in OSCC and may act as a tumor suppressor and genome guardian [36, 37]. PTEN also blocks the G1/S transition to prevent the malignant proliferation of cancer cells [38]. The defect of cell apoptosis facilitates the survival of neoplastic cells and plays a crucial role in tumor pathogenesis [39]. In this study, miR-103a-3p inhibition suppressed the proliferation of two OSCC cell lines as evidenced by decreased PCNA. Cells at the G1 phase were increased while cells at the S phase were reduced, suggesting that miR-103a-3p inhibition induced cell cycle
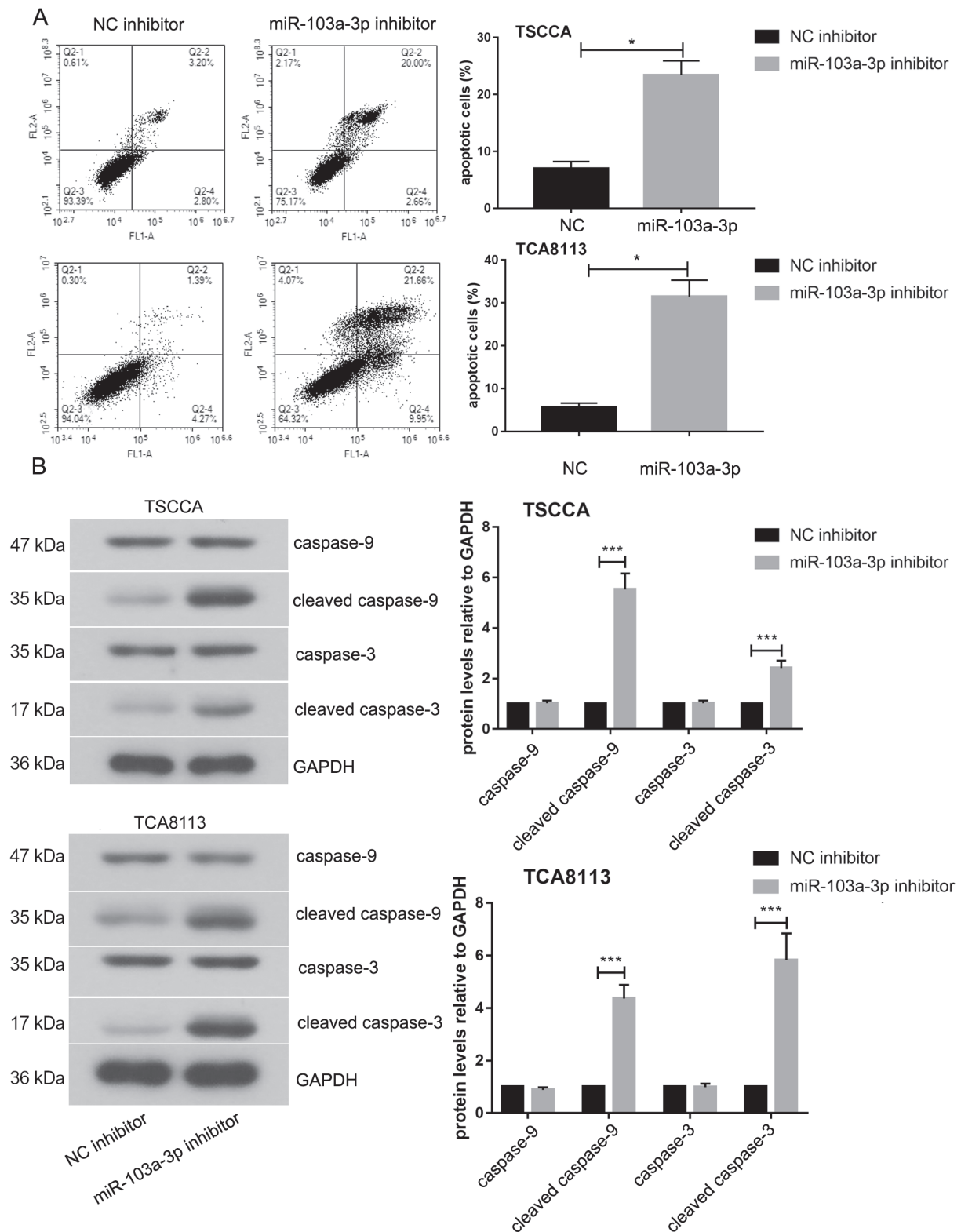
Figure 3. MiR-103a-3p inhibition promoted apoptosis of OSCC cell lines. A) TSCCA and TCA8113 cells were stained with Annexin V-FITC and propidium iodide after miR-103a-3p inhibition, cell apoptosis was detected by flow cytometry, and apoptotic cells were calculated (early apoptotic cells + late apoptotic cells). **B)** Protein levels of caspase-9, cleaved caspase-9, caspase-3, and cleaved caspase-3 in TSCCA and TCA8113 cells after miR-103a-3p inhibition were determined by the western blot assay. All data were presented as mean ± SD. *p<0.05; ***p<0.001
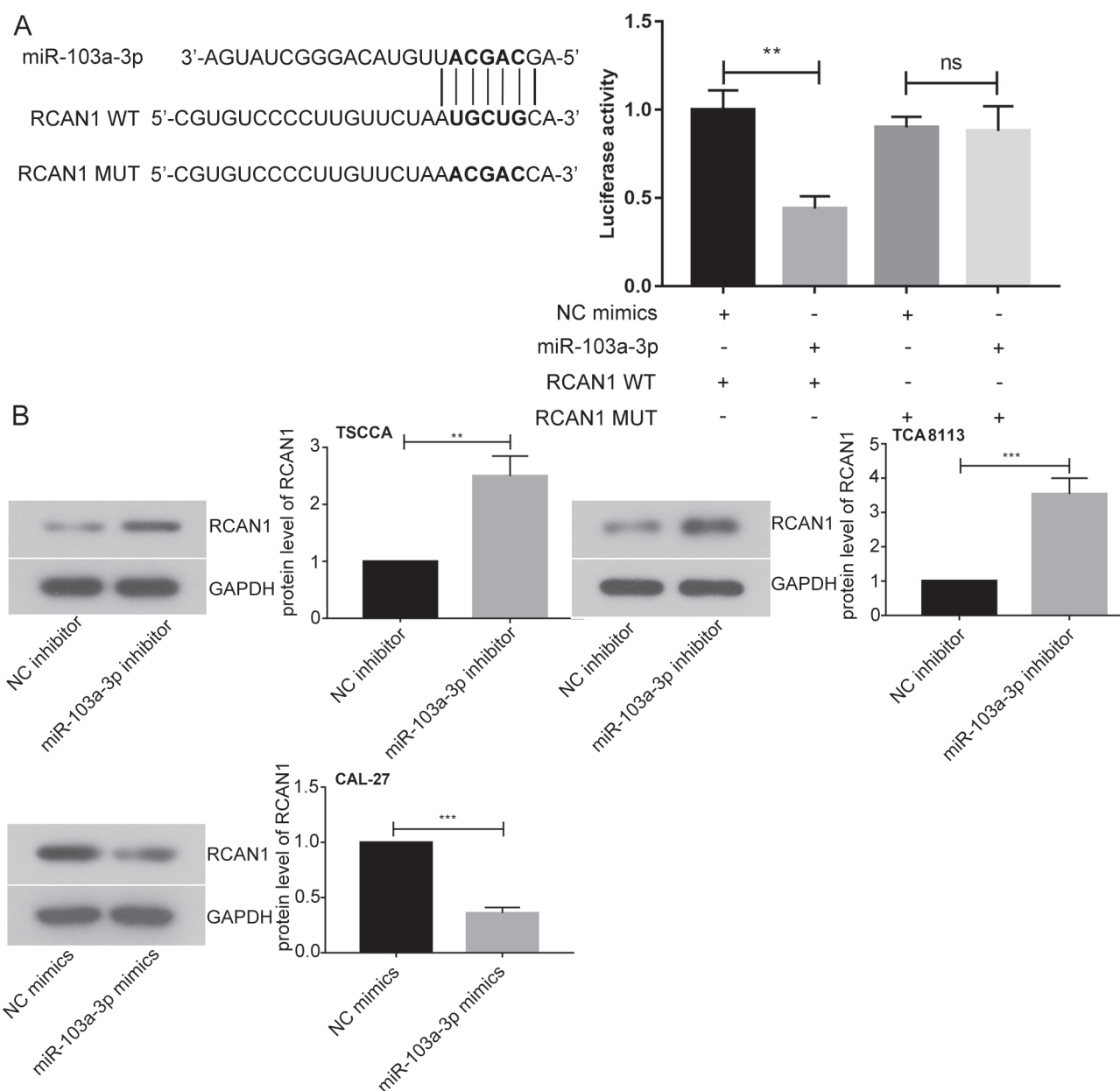
Figure 4. RCAN1 was a downstream target of miR-103a-3p. A) Specific binding site of miR-103a-3p on RCAN1 3'-UTR is displayed, and the correlation between miR-103a-3p and RCAN1 was validated by dual-luciferase assay. B) TSCCA and TCA8113 cells were transfected with NC inhibitor/miR-103a-3p inhibitor. CAL-27 cells were transfected with NC mimics/miR-103a-3p mimics. Protein level of RCAN1 was detected by the western blot assay. All data were presented as mean ± SD. ns: no significance; **p<0.01; ***p<0.001

arrest at the G1 phase, accompanied by decreased cyclin D1 and cyclin B1 expression. Elevated PTEN expression exacerbated the G1/S transition block, resulting in inhibited cell proliferation. Furthermore, miR-103a-3p inhibition induced apoptosis of OSCC cell lines. Late/early apoptotic cells were significantly increased, accompanied by elevated protein levels of cleaved caspase-9 and cleaved caspase-3, indicating that cell apoptosis signaling was activated after miR-103a-3p inhibition [40]. MiR-103a-3p antagomir also

inhibited tumor growth *in vivo*, suggesting its anti-tumor effect. In addition, we, for the first time, found a negative correlation between the expression levels of miR-103a-3p and RCAN1 in OSCC cell lines, and further dual-luciferase assay validated that RCAN1 is a downstream target of miR-103a-3p. By knocking down RCAN1 with its specific siRNA, cell proliferation was promoted and miR-103a-3p-induced cell cycle arrest was rescued. RCAN1 knockdown also reversed the miR-103a-3p mediated apoptosis
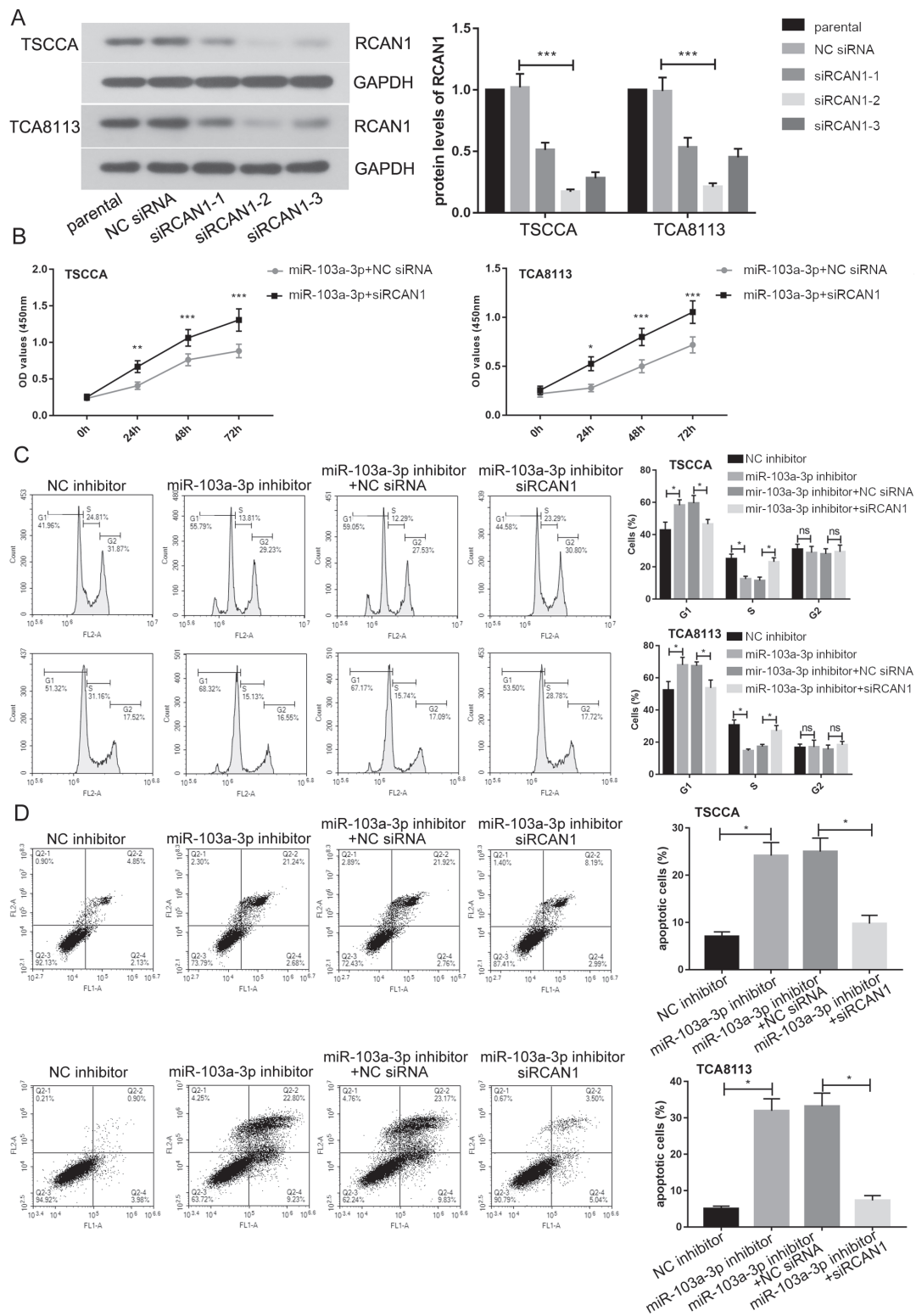
Figure 5. MiR-103a-3p regulated proliferation and apoptosis in the OSCC cell line by targeting RCAN1. A) RCAN1 expression was knocked down using specific RCAN1 siRNAs and the knockdown efficiency was evaluated by western blot assay. B) Proliferation of TSCCA and TCA8113 cells after RCAN1 silencing was assessed by cell counting kit-8 assay. C) Cell cycle after RCAN1 knockdown was assessed by flow cytometry assay. D) Apoptosis in TSCCA and TCA8113 cells after RCAN1 silencing was detected by flow cytometry. All data were presented as mean ± SD. ns: no significance; *p<0.05; **p<0.01; ***p<0.001
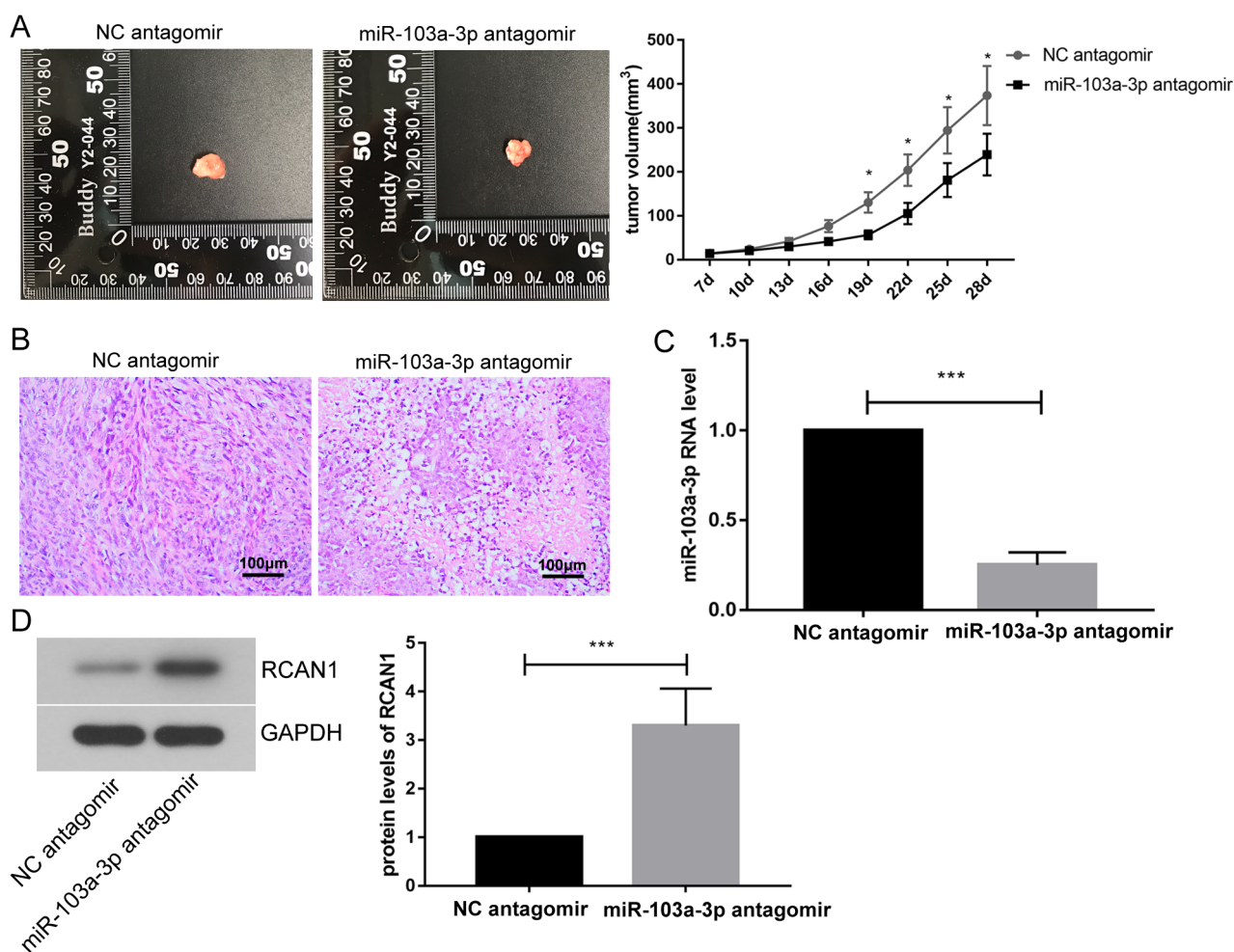
Figure 6. MiR-103a-3p inhibition suppressed tumor growth *in vivo*. A) Mice were implanted with TCA8113 cells and injected with NC/miR-103a-3p antagomir, tumor volume was recorded every three days. B) Pathophysiology of tumor tissues was assessed using hematoxylin-eosin staining assay. C) MiR-103a-3p level in tumor tissues was measured by quantitative real-time PCR. D) Protein level of RCAN1 in tumor tissues was determined by western blot assay. All data were presented as mean ± SD. *p<0.05; ***p<0.001

in OSCC cell lines. Numerous previous studies showed the anti-tumor effect of RCAN1. For instance, the expression of RCAN1 is repressed in human cancer cells and elevated RCAN1 level attenuated their malignancies including cell proliferation, migration, invasion and tumor angiogenesis [18]. To date, RCAN1 was found to suppress tumor growth both *in vivo* and *in vitro* through inhibiting the NF-κB signaling [41, 42]. Our study as the first proposed that RCAN1 is repressed by miR-103a-3p to further promote the proliferation of OSCC cell lines.

Salmena et al. proposed a "competitive endogenous RNA (ceRNA)" hypothesis in 2011, which demonstrated that messenger RNAs, transcribed pseudogenes and long non-coding RNAs can competitively bind to microRNAs via microRNA recognition elements (MRE) and further alleviated the target gene inhibition. And this regulatory

network plays crucial roles in numerous pathological conditions including cancer development [43]. In the present study, we found that LINC00675 overexpression resulted in the upregulation of miR-103a-3p targets RCAN1 and PTEN, suggesting that LINC00675 served as a sponge of miR-103a-3p in OSCC cells, and may act as an anti-tumor lncRNA. Our findings were highly consistent with a previous study, in which LINC00675 inhibits the proliferation and invasion of gastric cancer *in vitro* and suppresses tumor metastasis *in vivo* [44]. We may investigate the exact roles of LINC00675 in the migration, invasion, and metastasis of oral cancer in our future work.

In summary, our study demonstrated that miR-103a-3p inhibition suppressed the proliferation and induced apoptosis in OSCC cells through regulating RCAN1, and miR-103a-3p may be a novel diagnostic and therapeutic target for OSCC.
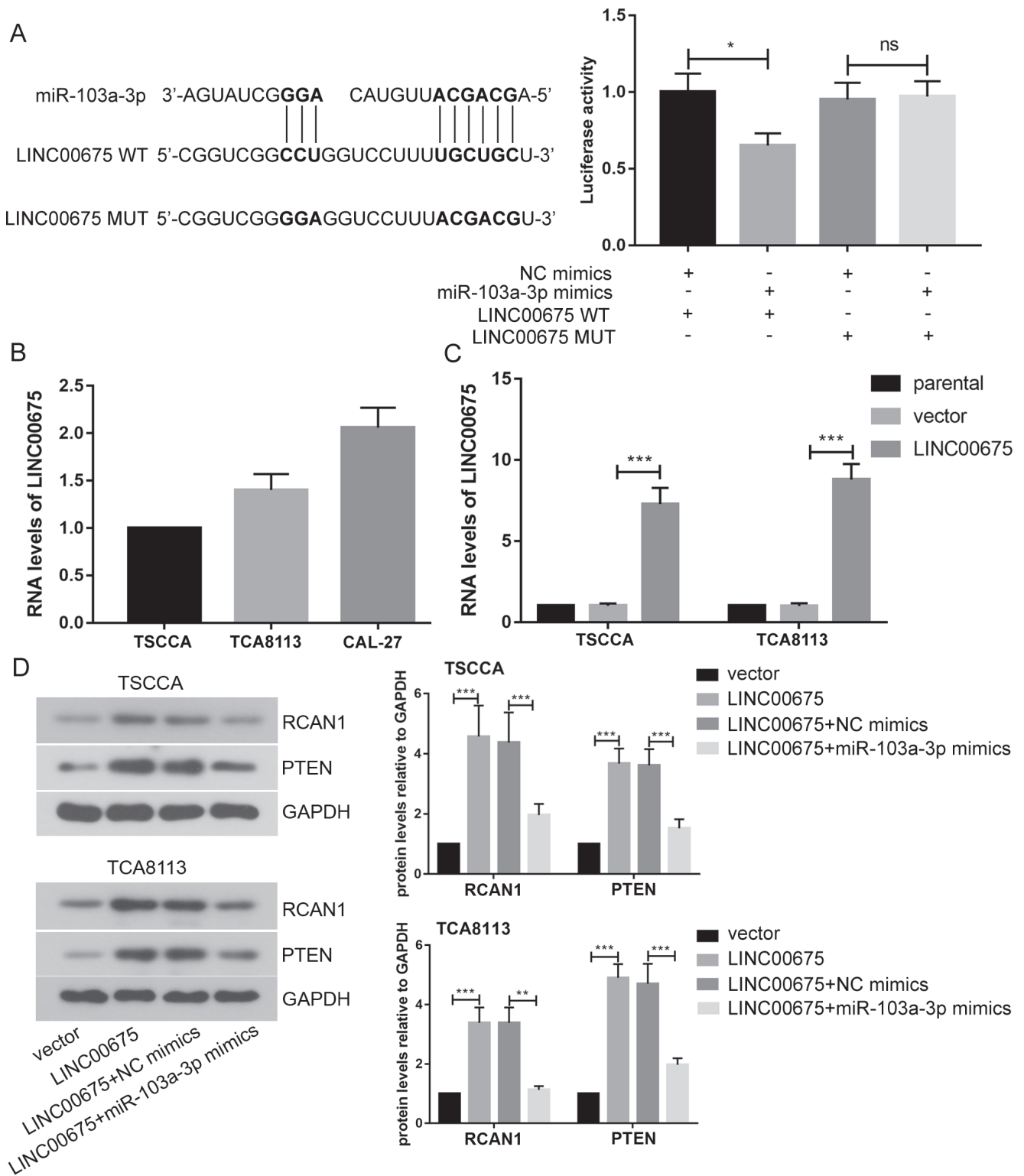
Figure 7. LINC00675 acted as a sponge of miR-103a-3p. A) The specific binding site of LINC00675 on miR-103a-3p was shown, and their correlation was validated by dual-luciferase assay. **B)** LINC00675 level was measured by quantitative real-time PCR. **C)** The over-expression efficiency of LINC00675 was evaluated by quantitative real-time PCR. **D)** TSCCA and TCA8113 cells were transfected with vector, LINC00675 over-expression plasmid, LINC00675 over-expression plasmid + NC mimics or LINC00675 over-expression plasmid + miR-103a-3p mimics, and protein levels of RCAN1 and PTEN were determined by western blot assay. All data were presented as mean ± SD. *p<0.05; **p<0.01; ***p<0.001

References

[1] SIEGEL RL, MILLER KD, JEMAL A. Cancer statistics, 2018. CA Cancer J Clin 2018; 68: 7–30. https://doi.org/10.3322/caac.21442

[2] VALDEZ JA, BRENNAN MT. Impact of Oral Cancer on Quality of Life. Dent Clin North Am 2018; 62: 143–154. https://doi.org/10.1016/j.cden.2017.09.001

[3] LINGEN MW, KALMAR JR, KARRISON T, SPEIGHT PM. Critical evaluation of diagnostic aids for the detection of oral cancer. Oral Oncol 2008; 44: 10–22. https://doi.org/10.1016/j.oraloncology.2007.06.011

[4] DISSANAYAKA WL, PITIYAGE G, KUMARASIRI PV, LI-YANAGE RL, DIAS KD et al. Clinical and histopathologic parameters in survival of oral squamous cell carcinoma. Oral Surg Oral Med Oral Pathol Oral Radiol 2012; 113: 518–525. https://doi.org/10.1016/j.oooo.2011.11.001

[5] SHARMA S, SATYANARAYANA L, ASTHANA S, SHIVALINGESH KK, GOUTHAM BS et al. Oral cancer statistics in India on the basis of first report of 29 population-based cancer registries. J Oral Maxillofac Pathol 2018; 22: 18–26. https://doi.org/10.4103/jomfp.JOMFP_113_17

[6] KOWALSKI LP, CARVALHO AL. Natural history of untreated head and neck cancer. Eur J Cancer 2000; 36: 1032–1037. https://doi.org/10.1016/s0959-8049(00)00054-x

[7] WILSON RC, DOUDNA JA. Molecular mechanisms of RNA interference. Annu Rev Biophys 2013; 42: 217–239. https://doi.org/10.1146/annurev-biophys-083012-130404

[8] CHANG JT, WANG F, CHAPIN W, HUANG RS. Identification of MicroRNAs as Breast Cancer Prognosis Markers through the Cancer Genome Atlas. PLoS One 2016; 11: e0168284. https://doi.org/10.1371/journal.pone.0168284

[9] JIANG X, DU L, WANG L, LI J, LIU Y et al. Serum microRNA expression signatures identified from genome-wide microRNA profiling serve as novel noninvasive biomarkers for diagnosis and recurrence of bladder cancer. Int J Cancer 2015; 136: 854–862. https://doi.org/10.1002/ijc.29041

[10] DAUGAARD I, VENO MT, YAN Y, KJELDSEN TE, LAMY P et al. Small RNA sequencing reveals metastasis-related microRNAs in lung adenocarcinoma. Oncotarget 2017; 8: 27047–27061. https://doi.org/10.18632/oncotarget.15968

[11] CARITG O, NAVARRO A, MORENO I, MARTINEZ-RODE-NAS F, CORDEIRO A et al. Identifying High-Risk Stage II Colon Cancer Patients: A Three-MicroRNA-Based Score as a Prognostic Biomarker. Clin Colorectal Cancer 2016; 15: e175–e182. https://doi.org/10.1016/j.clcc.2016.04.008

[12] HU X, MIAO J, ZHANG M, WANG X, WANG Z et al. miRNA-103a-3p Promotes Human Gastric Cancer Cell Proliferation by Targeting and Suppressing ATF7 in vitro. Mol Cells 2018; 41: 390–400. https://doi.org/10.14348/molcells.2018.2078

[13] WEBER DG, CASJENS S, JOHNEN G, BRYK O, RAIKO I et al. Combination of MiR-103a-3p and mesothelin improves the biomarker performance of malignant mesothelioma diagnosis. PLoS One 2014; 9: e114483. https://doi.org/10.1371/journal.pone.0114483

[14] ZHOU H, RIGOUTSOS I. MiR-103a-3p targets the 5' UTR of GPRC5A in pancreatic cells. RNA 2014; 20: 1431–1439. https://doi.org/10.1261/rna.045757.114

[15] BERANIA I, CARDIN GB, CLEMENT I, GUERTIN L, AYAD T et al. Four PTEN-targeting co-expressed miRNAs and ACTN4- targeting miR-548b are independent prognostic biomarkers in human squamous cell carcinoma of the oral tongue. Int J Cancer 2017; 141: 2318–2328. https://doi.org/10.1002/ijc.30915

[16] CHAN B, GREENAN G, MCKEON F, ELLENBERGER T. Identification of a peptide fragment of DSCR1 that competitively inhibits calcineurin activity in vitro and in vivo. Proc Natl Acad Sci U S A 2005; 102: 13075–13080. https://doi.org/10.1073/pnas.0503846102

[17] SONG Z, CAO Q, RUAN H, YANG H, WANG K et al. RCAN1.4 acts as a suppressor of cancer progression and sunitinib resistance in clear cell renal cell carcinoma. Exp Cell Res 2018; 372: 118–128. https://doi.org/10.1016/j.yexcr.2018.09.017

[18] MA N, SHEN W, PANG H, ZHANG N, SHI H et al. The effect of RCAN1 on the biological behaviors of small cell lung cancer. Tumour Biol 2017; 39: 1010428317700405. https://doi.org/10.1177/1010428317700405

[19] HASLE H, CLEMMENSEN IH, MIKKELSEN M. Risks of leukaemia and solid tumours in individuals with Down's syndrome. Lancet 2000; 355: 165–169. https://doi.org/10.1016/S0140-6736(99)05264-2

[20] MARTIN-MARTIN L, LOPEZ A, VIDRIALES B, CABALLERO MD, RODRIGUES AS et al. Classification and clinical behavior of blastic plasmacytoid dendritic cell neoplasms according to their maturation-associated immunophenotypic profile. Oncotarget 2015; 6: 19204–19216. https://doi.org/10.18632/oncotarget.4146

[21] LIN SR, YANG HC, KUO YT, LIU CJ, YANG TY et al. The CRISPR/Cas9 System Facilitates Clearance of the Intrahepatic HBV Templates In Vivo. Mol Ther Nucleic Acids 2014; 3: e186. https://doi.org/10.1038/mtna.2014.38.

[22] KO SC, HUANG CR, SHIEH JM, YANG JH, CHANG WC et al. Epidermal growth factor protects squamous cell carcinoma against cisplatin-induced cytotoxicity through increased interleukin-1beta expression. PLoS One 2013; 8: e55795. https://doi.org/10.1371/journal.pone.0055795

[23] HOU G, XUE L, LU Z, FAN T, TIAN F et al. An activated mTOR/p70S6K signaling pathway in esophageal squamous cell carcinoma cell lines and inhibition of the pathway by rapamycin and siRNA against mTOR. Cancer Lett 2007; 253: 236–248. https://doi.org/10.1016/j.canlet.2007.01.026

[24] YU J, PENG Y, WU LC, XIE Z, DENG Y et al. Curcumin down-regulates DNA methyltransferase 1 and plays an antileukemic role in acute myeloid leukemia. PLoS One 2013; 8: e55934. https://doi.org/10.1371/journal.pone.0055934

[25] ABDOU HS, ATLAS E, HACHE RJ. Liver-enriched inhibitory protein (LIP) actively inhibits preadipocyte differentiation through histone deacetylase 1 (HDAC1). J Biol Chem 2011; 286: 21488–21499. https://doi.org/10.1074/jbc.M110.211540

[26] LI LN, XIAO T, YI HM, ZHENG Z, QU JQ et al. MiR-125b Increases Nasopharyngeal Carcinoma Radioresistance by Targeting A20/NF-kappaB Signaling Pathway. Mol Cancer Ther 2017; 16: 2094–2106. https://doi.org/10.1158/1535-7163.MCT-17-0385

[27] CERVIGNE NK, REIS PP, MACHADO J, SADIKOVIC B, BRADLEY G et al. Identification of a microRNA signature associated with progression of leukoplakia to oral carcinoma. Hum Mol Genet 2009; 18: 4818–4829. https://doi.org/10.1093/hmg/ddp446

[28] YU ZW, ZHONG LP, JI T, ZHANG P, CHEN WT et al. MicroRNAs contribute to the chemoresistance of cisplatin in tongue squamous cell carcinoma lines. Oral Oncol 2010; 46: 317–322. https://doi.org/10.1016/j.oraloncology.2010.02.002

[29] MURUGAN AK, MUNIRAJAN AK, ALZAHRANI AS. MicroRNAs: Modulators of the Ras Oncogenes in Oral Cancer. J Cell Physiol 2016; 231: 1424–1431. https://doi.org/10.1002/jcp.25269

[30] SAMPSON VB, RONG NH, HAN J, YANG Q, ARIS V et al. MicroRNA let-7a down-regulates MYC and reverts MYC-induced growth in Burkitt lymphoma cells. Cancer Res. 2007; 67: 9762–9770. https://doi.org/10.1158/0008-5472.CAN-07-2462

[31] SHIN KH, BAE SD, HONG HS, KIM RH, KANG MK et al. miR-181a shows tumor suppressive effect against oral squamous cell carcinoma cells by downregulating K-ras. Biochem Biophys Res Commun 2011; 404: 896–902. https://doi.org/10.1016/j.bbrc.2010.12.055

[32] SALAZAR C, NAGADIA R, PANDIT P, COOPER-WHITE J, BANERJEE N et al. A novel saliva-based microRNA biomarker panel to detect head and neck cancers. Cell Oncol (Dordr) 2014; 37: 331–338. https://doi.org/10.1007/s13402-014-0188-2

[33] OTTO T, SICINSKI P. Cell cycle proteins as promising targets in cancer therapy. Nat Rev Cancer 2017; 17: 93–115. https://doi.org/10.1038/nrc.2016.138

[34] RAMOS-GARCIA P, GIL-MONTOYA JA, SCULLY C, AYEN A, GONZALEZ-RUIZ L et al. An update on the implications of cyclin D1 in oral carcinogenesis. Oral Dis 2017; 23: 897–912. https://doi.org/10.1111/odi.12620

[35] KUSHNER J, BRADLEY G, YOUNG B, JORDAN RC. Aberrant expression of cyclin A and cyclin B1 proteins in oral carcinoma. J Oral Pathol Med 1999; 28: 77–81. https://doi.org/10.1111/j.1600-0714.1999.tb02000.x

[36] ALI IU, SCHRIML LM, DEAN M. Mutational spectra of PTEN/MMAC1 gene: a tumor suppressor with lipid phosphatase activity. J Natl Cancer Inst 1999; 91: 1922–1932. https://doi.org/10.1093/jnci/91.22.1922

[37] PEI LJ, LI JD, ZHAO ZH, LI J, LIANG RY et al. [Effect of triptolide on human oral cancer cell proliferation and PTEN gene mRNA expression in oral cancer]. Zhonghua Kou Qiang Yi Xue Za Zhi 2017; 52: 44–47. https://doi.org/10.3760/cma.j.issn.1002-0098.2017.01.009

[38] BRANDMAIER A, HOU SQ, SHEN WH. Cell Cycle Control by PTEN. J Mol Biol 2017; 429: 2265–2277. https://doi.org/10.1016/j.jmb.2017.06.004

[39] HASSAN M, WATARI H, ABUALMAATY A, OHBA Y, SAKURAGI N. Apoptosis and molecular targeting therapy in cancer. Biomed Res Int 2014; 2014: 150845. https://doi.org/10.1155/2014/150845

[40] BRENNER D, MAK TW. Mitochondrial cell death effectors. Curr Opin Cell Biol 2009; 21: 871–877. https://doi.org/10.1016/j.ceb.2009.09.004

[41] LIU C, ZHENG L, WANG H, RAN X, LIU H et al. The RCAN1 inhibits NF-kappaB and suppresses lymphoma growth in mice. Cell Death Dis 2015; 6: e1929. https://doi.org/10.1038/cddis.2015.260

[42] CHEN X, HU Y, WANG S, SUN X. The regulator of calcineurin 1 (RCAN1) inhibits nuclear factor kappaB signaling pathway and suppresses human malignant glioma cells growth. Oncotarget 2017; 8: 12003–12012. https://doi.org/10.18632/oncotarget.14479

[43] SALMENA L, POLISENO L, TAY Y, KATS L, PANDOLFI PP. A ceRNA hypothesis: the Rosetta Stone of a hidden RNA language? Cell 2011; 146: 353–358. https://doi.org/10.1016/j.cell.2011.07.014

[44] ZENG S, XIE X, XIAO YF, TANG B, HU CJ et al. Long noncoding RNA LINC00675 enhances phosphorylation of vimentin on Ser83 to suppress gastric cancer progression. Cancer Lett 2018; 412: 179–187. https://doi.org/10.1016/j.canlet.2017.10.026